Journal of Sustainability Science and Management Special Issue Number 2: Fundamental Interdisciplinary Pathways To Future Sustainability 2017: 16-26
ISSN: 1823-8556
© Penerbit UMT

GROWTH AND CHARACTERIZATION OF MULTI-WALLED CARBON NANOTUBES USING Ni-MCM41 MESOPOROUS CATALYST AND THEIR APPLICATION AS ADSORBENT

AMIRAH AHMAD, MOHD HASMIZAM RAZALI AND KHAIRUL ANUAR MAT AMIN*

Advanced Nanomaterials Research Group, School of Fundamental Science, Universiti Malaysia Terengganu, 21030 Kuala Nerus, Terengganu, Malaysia.

**Corresponding author: kerol@umt.edu.my*

Abstract: Carbon nanotubes (CNTs) are employed by chemical vapour deposition (CVD) method using Ni-MCM41 mesoporous as a catalyst. Ni-MCM41 mesoporous catalysts are synthesised by nickel's incorporation into the MCM41 framework through hydrothermal method, using sodium metasilicate as silica source and cetyltrimethylammonium bromide as a template. The powder X-ray diffraction (XRD) and Fourier transform infrared spectroscopy (FTIR) results confirmed the synthesised CNTs grown on the Ni-MCM41 catalyst are multi-walled carbon nanotubes (MWNTs). Scanning electron microscopy micrograph of synthesised CNTs showed the hairlike structure with the diameter in between 2-5 nm and a few hundred nanometres in length. The synthesised CNTs are tested as an adsorbent for methyl orange removal in aqueous solution. Results show that 98 % of methyl orange is removed by synthesised CNTs after 1 hour of reaction and comparable to commercial MWNTs at 100 %. This study shows that the synthesised CNTs have a great potential to be used as an adsorbent for methyl orange removal.

Keywords: Carbon nanotubes, chemical vapor deposition, mesoporous, adsorbent

Introduction

Nowadays, many researchers are studying dye removal from water due to the toxicity and carcinogenic effects of the latter. These pollutants come from various industries, especially from the textile sector which greatly threatens the human population's health and the natural ecosystem. Several methods are employed in removing the dye materials from contaminated water, such as physical, chemical and biological methods. Among these methods, adsorption methods are reasonable methods because of its economic, high efficiency, operation and feasibility (Belay & Hayelom, 2014). Various adsorption materials have been used for dye's removal such as activated carbon (Kobya *et al*., 2005), biomaterials (Minamisawa *et al*., 2004), clay (Potgieter *et al*., 2006), lignocellulose materials (Demirbas, 2008) and carbon nanotubes (Gong *et al*., 2009). Based on previous studies, activated carbon is the most effective adsorbent due to its structural characteristics and porous structure which provides a large surface area and can be easily modified to increase their properties. However, these materials have many drawbacks due to their low loading capacities, relatively weak interactions with dyes and expensive cost (Pal *et al*., 2013).

Carbon nanotubes (CNTs) have also aroused widespread attention as promising adsorbents due to their outstanding ability for the removal of various inorganic and organic pollutants. It has also offered high mechanical strength, thermal conductivity and unique electronic properties (Wildgoose *et al*., 2006). However, CNTs size selectivity has been hampered because of their uncontrolled diameters and random growth direction in the pores of the substrate. It occurred due to lack of uniform pore size catalyst distribution (Che *et al*., 1998). MCM41 has a high surface area and thin amorphous silica walls, thereby allowing the pore size to be varied from 2 – 10 nm and its chemical properties can be manipulated to CNTs selectivity. Hence, MCM41 material

with fixed pore size precisely controls the pore size and CNTs growth direction (Duxiao *et al*., 2001). The CNTs controlled growth is important to avoid these clusters aggregation into large particles during the high-temperature reaction. Study on the growth of single-walled carbon nanotubes over Co-MCM41 mesoporous molecular sieves reported that SWNTs with a diameter up to 35 nm was successfully grown on Co-MCM41 (Somanathan *et al*., 2006). A better thermal stability and high productivity observed suggest that the mesoporous molecular sieves could be a synthesizing catalytic template for CNTs (Herrera *et al*., 2001).

In this study, the carbon nanotubes (CNTs) were synthesized by using nickel (Ni) loaded on a mesoporous MCM41 (Ni-MCM41) catalyst. Sulphuric and nitric acid mixtures were used in removing catalyst and to treat the surface of CNTs obtained. Surface treatment improves CNTs dispersion in aqueous and decreases aggregate formation. Besides, the CNTs adsorption capacity can be increased after treatments due to the oxygen presence containing functional groups at the surface. The defects also generated by the CNTs chemical treatment. These functional groups and defects act as active sites which are easily accessible to the dye molecules (Gupta *et al*., 2013). The synthesized CNTs were then tested as an adsorbent material for methyl orange removal.

Material and Methods

Materials

Sodium metasilicate (Na_2SiO_3) was purchased from Sigma Aldrich, St Louis, Missouri, USA. N-hexadecyl trimethyl ammonium bromide (CTABr) and nickel nitrate hexahydrate (Ni $(NO_3)_2 6H_2O$) were obtained from Merck, Malaysia. Methyl orange ($C_{14}H_{14}N_3NaO_3S$) was obtained from Fisher Scientific, UK. All chemicals were used as received without further purification steps taken.

Synthesis of Mesoporous Ni-MCM41 Catalyst

The mesoporous Ni-MCM41 synthesis was carried out according to the Na_2SiO_3 molar composition: Ni $(NO_3)_2$: 0.2 CTAB: 120 H_2O. Sodium metasilicate and nickel nitrate were dissolved in distilled water and stirred for 1 hour. The pH of the mixtures was then adjusted to ~10.5 by adding 1M sulphuric acid. The aqueous solutions of CTAB were added into the mixture and simultaneously stirred vigorously for 1 hour at room temperature. The resulting mixtures were autoclaved and heated at 145 °C for 48 hours. Then, the mixtures were filtered, washed several times with distilled water and oven dried at 80 °C for 3 hours. Finally, the products were calcined at 550 °C in the furnace for 6 hours to remove the surfactant.

Preparation of CNTs

CNTs were prepared using chemical vapour deposition (CVD) method. The 0.1 g of Ni-MCM41 catalyst in a quartz plate was placed into a hollow tube furnace and heated to 600 °C. Then, acetylene gas was introduced into the tube for 10 minutes. After the reactions were completed, the flow of acetylene was stopped and the samples were allowed to cool to room temperature. The CNTs were obtained as a black solid. For purification, the grown CNTs were added into the sulphuric acid mixture (5 M) and nitric acid (5 M) at the ratio 3:1. The mixtures were refluxed for 3 hours at 100 °C. Then, the mixtures were filtered, washed with distilled water and dried at 60 °C for 24 hours.

Characterizations

For low-angle, X-ray diffractograms were obtained using Bruker D8 Advance with Cu Kα radiation with λ = 0.154 nm at 40 kV and 40 mA. Samples were measured in the range of 2θ from 0° to 10°. For high-angle, X-ray diffractograms were acquired by using Rigaku D/max-2500 powder diffractometer with Cu-Kα source (λ = 0.154 nm, 40 kV, 40mA) and operating at a scanning rate of 2.00^0 min^{-1}. The diffraction

spectra were recorded at the diffraction angle, 2θ from 10^0 to 80^0 at room temperature, with a 10° step size interval. The FTIR spectra were acquired by using Perkin Elmer 1650 Infrared Spectrometer. The technique used for FTIR analysis was potassium bromide (KBr) pellets. The samples were characterized by particle size and morphology using a Scanning Electron Microscope JOEL JSM-6360LA with the energy 15 kV couple with EDX analyser.

Adsorption study

Methyl orange (MO) dyes were used to prepare the stock solution (1000 ppm) in distilled water. The solutions were prepared by diluting the stock solution in distilled water. Then, 0.01 g of the synthesized CNTs was thoroughly mixed in 100 ml of the dye solution (20 ppm). The mixtures were shaken at 200 rpm using the shaker for 60 minutes. The effluents were collected after 10, 20, 30 and 60 minutes. The MO concentration was measured by UV-Vis Spectrophotometer Shimadzu UV-1800 and analyzed with UV-Probe software (version 2.43). The resulting absorbance values were compared to the MO concentration absorbed via a constructed standard curve used to calculate the percentage removal of the samples. The removal (%) was calculated according to the following equation:

$$\%\,removal = \frac{(C_i - C_f)}{C_i} x\,100$$

where C_f and C_i represent the initial and final dye solution concentrations (mg L-1), respectively.

Results and Discussion

Synthesis Ni-MCM41 Catalyst

Figure 1 shows the XRD patterns of low angle uncalcined and calcined Ni-MCM41 as well as high angle Ni-MCM41, respectively. The three

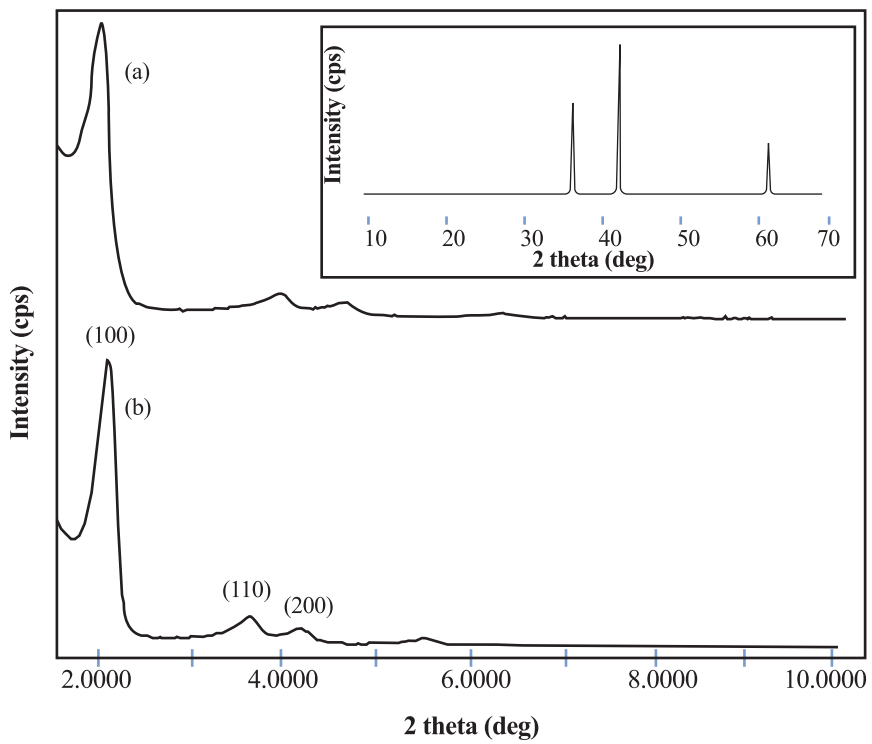


Figure 1: XRD patterns of (a) uncalcined Ni-MCM41 and (b) calcined Ni-MCM41. The inset picture shows the high-angle XRD result of the Ni-MCM41 catalyst.

peaks at (100), (110) and (200) of the latter show the typical characteristics of MCM41 hexagonal ordered structures (Occelli *et al*., 1999). It indicates that the Ni-MCM41 catalyst has hexagonal pores with long order framework. For the uncalcined Ni-MCM41, a strong (100) peak in between 2θ = 1.5° - 2.5° was seen and this peak was increased after calcination due to the removal of surfactant template. This can lead to the rearrangement MCM41 silica walls thus increase the MCM41 crystallinity (Taib *et al*., 2011). The high peak of calcined Ni-MCM41 indicates that Ni-MCM41 with a higher long range degree ordered framework and well-formed hexagonal structures was successfully synthesized.

Previous study also reported that these three peaks show the intense diffraction peak in the range 1.8 to 2.2 (2θ) due to (100) plane and 2 small peaks which were (110) and (200) plane confirming the materials hexagonal mesophase (Tangestaninejad *et al*., 2009). While, the three sharp and narrow peaks at 2θ values of 37.24, 43.27 and 62.87° with d values of 2.41, 2.09 and 1.48 Å (Figure 1 (inset)) assigned to cubic NiO phase. These peaks indicate that nickel was successfully added into MCM41.

Figure 2 displays the FTIR spectra of Ni-MCM41 uncalcined and Ni-MCM41 calcined, respectively. The two sharp peaks observed at 2921 cm^{-1} and 2851 cm^{-1} confirms the presence of asymmetric C-H and symmetric C-H vibrations of the surfactants. After calcination, these 2 peaks disappeared due to the removal of surfactant. It is suggested that the surfactant template was successfully removed from the MCM41 framework. The major MCM41 peak also observed in samples which have the bands around 1026 cm^{-1}, 707 cm^{-1} and 471 cm^{-1} assigned to Si-O-Si asymmetry, Si-O-So symmetry and Si-O-Si bending, respectively. All these peaks observed were found to be similar in other work related to MCM41 material (Scheibe *et al*., 2009).

Figure 3 presents the SEM images of (a) MCM41, (b) Ni-MCM41 and (c) elemental image and Ni-MCM41 catalyst data analysis.

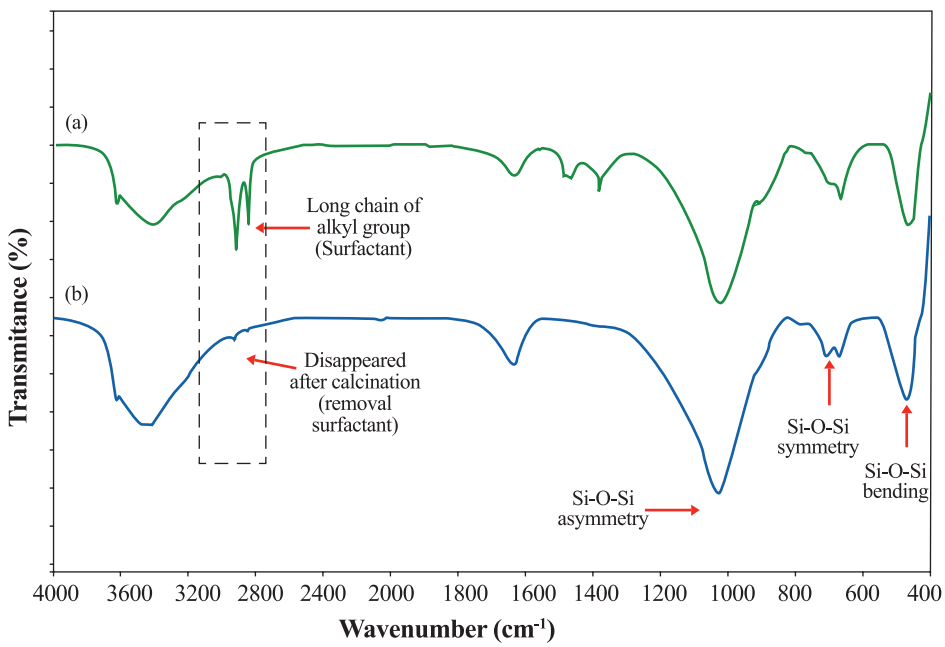


Figure 2: FTIR spectra of (a) uncalcined Ni-MCM41 and (b) calcined Ni-MCM41 catalyst

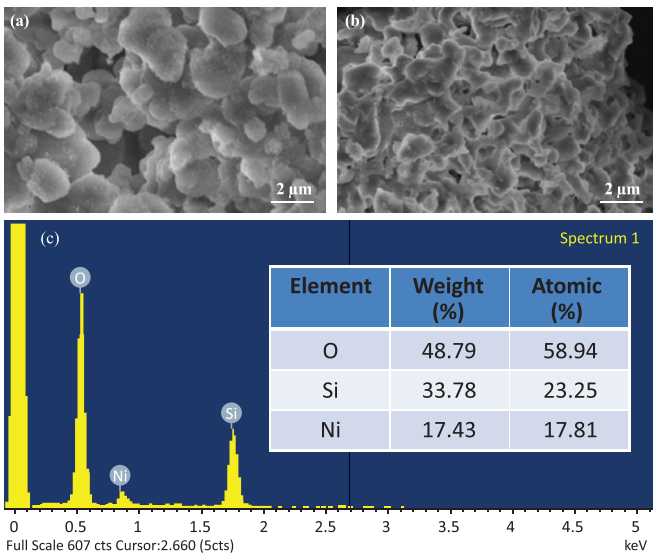


Figure 3: Scanning electron microscopy images of (a) MCM41 and (b) Ni-MCM41,and (c) EDX image and data analysis of Ni-MCM41 catalyst

The micrograph shows that MCM41 catalyst has an agglomerated spherical particle in between 1 to 3 µm in diameter. For Ni-MCM41, the image displays the prepared catalyst as a 'worm' type with irregular shape particles. Ni-MCM41 possess different morphology and the MCM41 structurally changed upon immobilization. The existence of nickel in the Ni-MCM41 catalyst is shown by the EDX image (Figure 3c).

CNT Grown on Ni-MCM41

Figure 4 (a) shows the XRD patterns of unpurified and purified CNTs grown on the Ni-

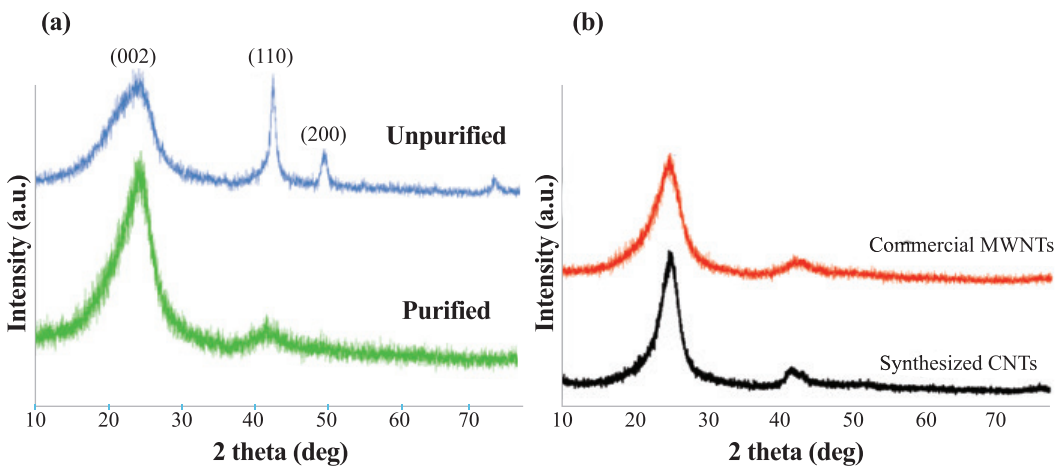


Figure 4: XRD patterns of (a) unpurified and purified CNTs grown on Ni-MCM41 and (b) comparison of commercial multi-walled carbon nanotubes (MWNTs) and synthesized CNTs grown on the Ni-MCM41 catalyst

MCM41 catalyst. The peak at (002) indicates the hexagonal graphite and the two peaks at (110) and (200) were attributed to the catalytic impurities (Krishnamurthy & Namitha, 2013; Masoumi *et al*., 2010). After the successful CNTs purification process, the two peaks at (110) and (200) were almost disappearing and indicating the catalytic impurities removal from the CNTs surface. To confirm the types of synthesized CNTs obtained, the XRD results were compared with commercial multi-walled carbon nanotubes (Figure 4 (b)). The results clearly show that our synthesized CNTs were similar to the commercial multi-walled carbon nanotube pattern. Figure 5 shows the Raman unpurified spectra and purified CNTs grown on Ni-MCM41, along with commercial MWNTs, respectively. The results confirmed that the synthesized CNTs are multi-walled due to the absence of a radial breathing mode (RBM) peak in the range of 100 cm^{-1} to 350 cm^{-1} (Masoumi *et al*., 2010). The two peaks are detected at ~1340 cm^{-1} and ~1580 cm^{-1} corresponding to D and G bands, respectively (Sheikh *et al*., 2015). The D band is attributed to the disordered CNTs graphite structure and the G band is assigned to the C=C bond in the graphite. The quality of synthesized CNTs can be supported by measuring the intensity ratio of the D band to the G band (ID/IG) to determine the number of defects on the sidewalls of CNTs (Murphy *et al*., 2006). In this study, the ID/IG ratio was found to increase from 0.90 for unpurified CNTs to 1.31 after purification, thus explained that the purification possessed more carbon-containing defects and less graphitized as compared to the unpurified CNTs. As for comparison purposes, the ID/IG ratio for purified CNTs grown on Ni-MCM41 was compared with commercial MWNTs (use in this study). The result shows that the ID/IG value for CNTs grown on commercial MWNTs is 1.21 and purified CNTs grown on Ni-MCM41 recorded at 1.31 (ID/IG=1.31) (Figure 5(c)). From these ratio values, the commercial MWNTs have lesser carbon-containing defects and much graphitized structure than our purified CNTs.

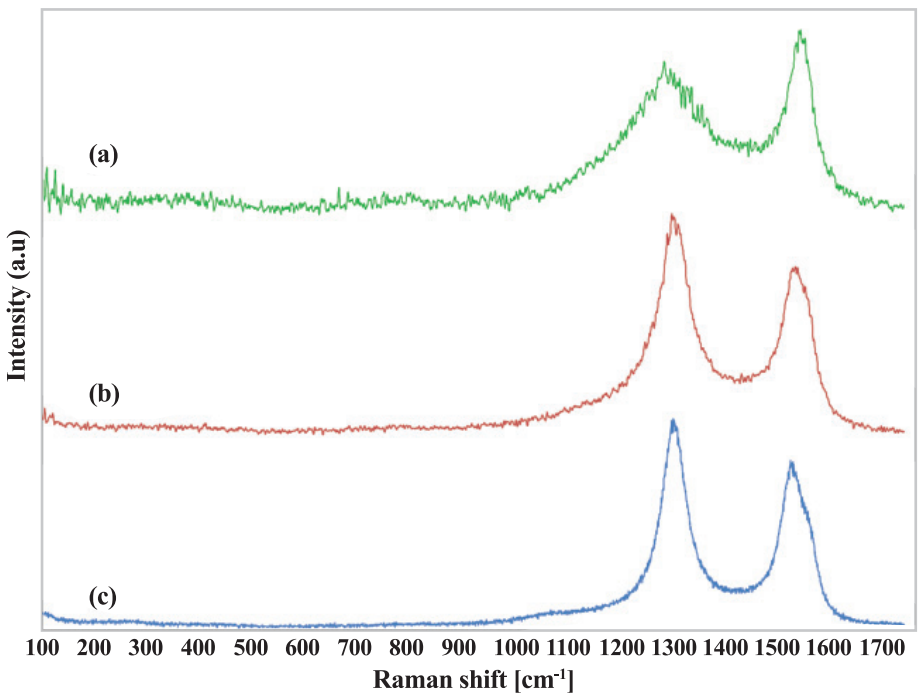


Figure 5: Raman spectra of (a) unpurified CNTs grown on Ni-MCM41, (b) purified CNTs grown on Ni-MCM41 and (c) commercial MWNTs

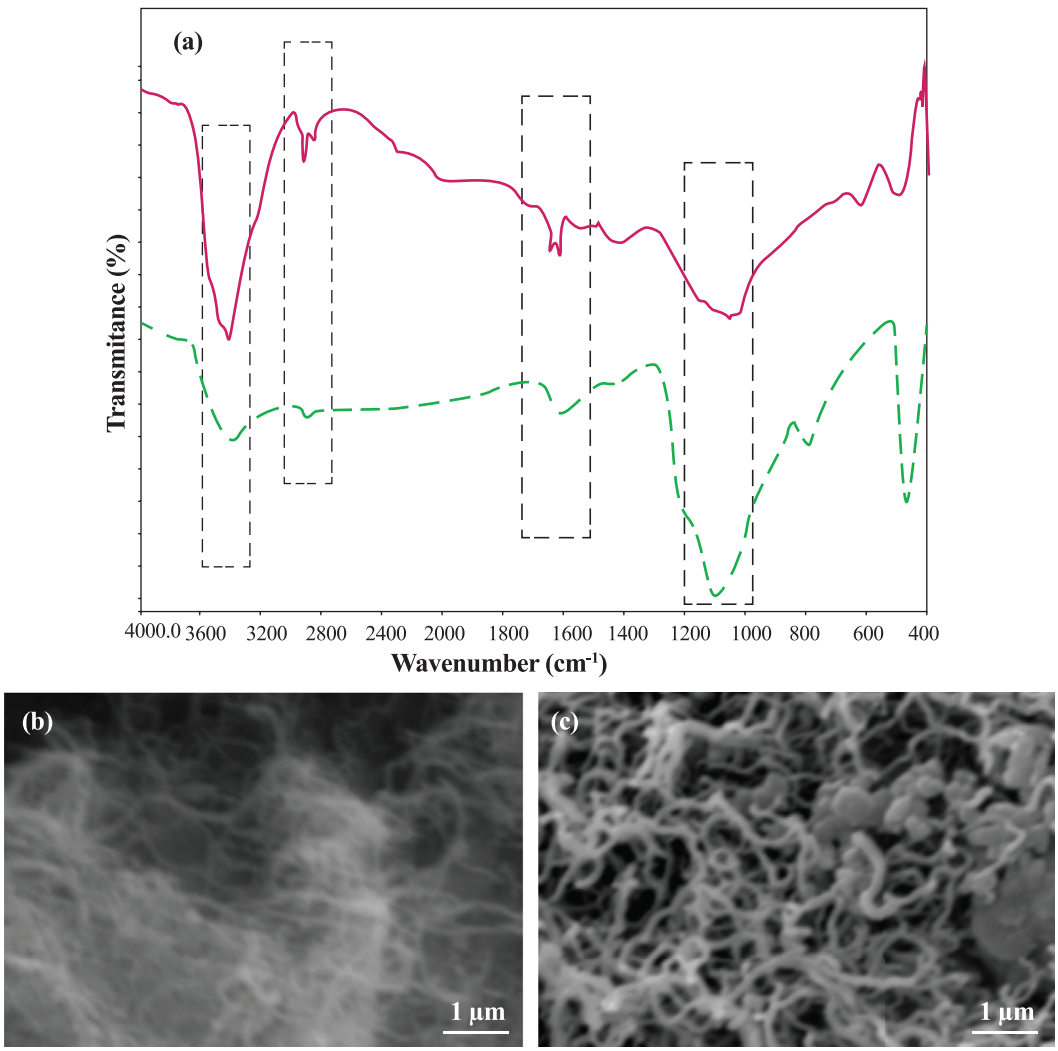


Figure 6: (a) FTIR spectra of the commercial multi-walled carbon nanotubes (straight line) and synthesized CNTs (dash line), SEM micrograph of (b) commercial MWNTs and (c) synthesized CNTs grown on Ni-MCM41 catalyst

Figure 6 (a) displays the FTIR spectra of synthesized CNTs and commercial MWNTs, respectively. Both samples exhibit similar patterns which the major peaks of commercial multi-walled CNTs are observed around 3400 cm^{-1} corresponding to O-H groups, two bands around 2950 cm^{-1} and 2850 cm^{-1} assigned to C-H groups, band around ~1680 cm^{-1} corresponding to C=C and a broadband between 1050 cm^{-1} to 1300 cm^{-1} attributed to C-O groups due to defective sites during the purification process.

All these important peaks observed in the FTIR spectra of synthesized CNTs grown on the Ni-MCM41 catalyst. The previous study reported that the FTIR spectra were used to confirm the defective sites at the CNTs surface during purification with the presence of C=C, C=O, CH2 and OH functional groups (Mishra *et al*., 2010). The SEM images also show our synthesized CNTs appearing as a hair-like structure with the diameter in between 2 to 5 nm and a few hundred nanometres in lengths (Figure 6 (c)).

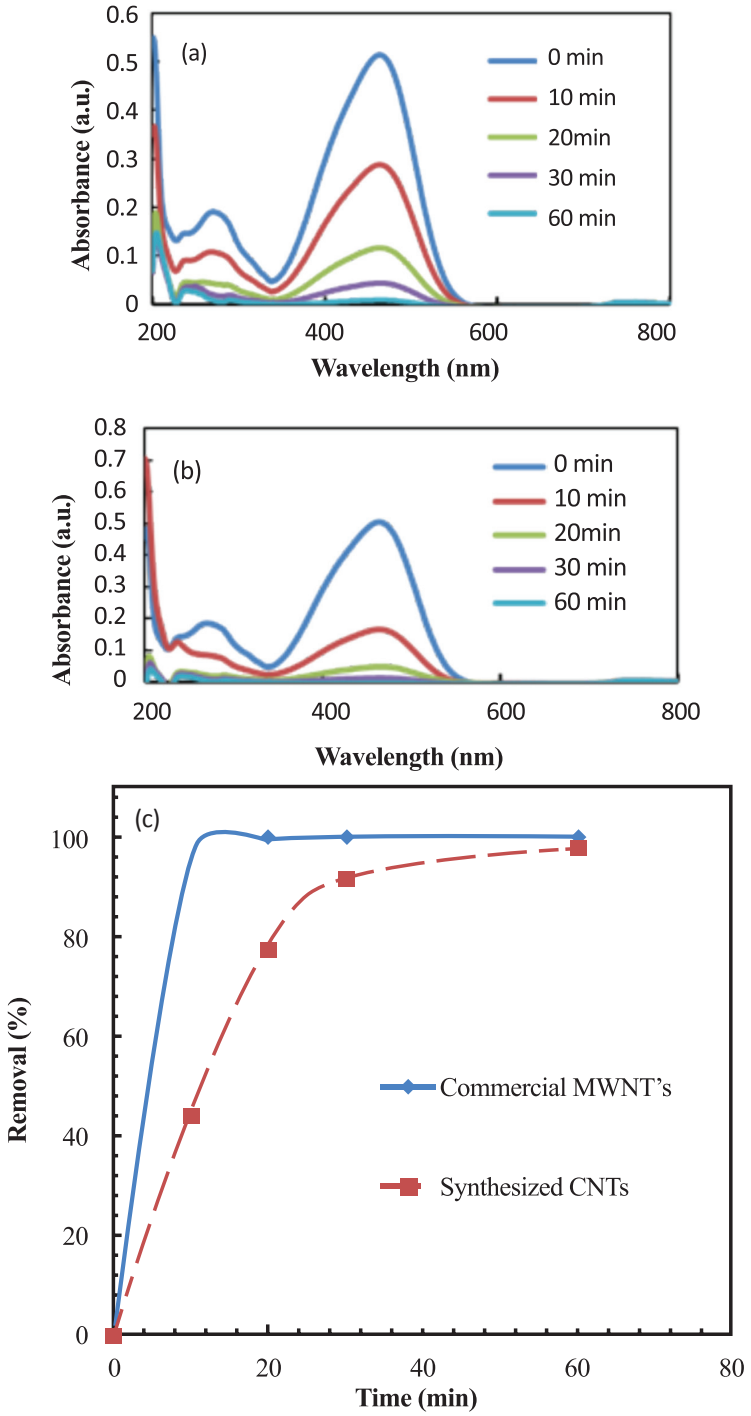


Figure 7: UV-Vis spectrum for methyl orange adsorption using (a) synthesized CNTs, (b) commercial multi-walled carbon nanotubes (MWNTs) and (c) methyl orange percentage removal using commercial MWNTs and synthesized CNTs as adsorbents

Adsorption activity

Figure 7 shows the UV-Vis spectrum for adsorption of methyl orange using synthesized CNTs and commercial CNTs, respectively (Figure 7 (a and b)). The methyl orange specific wavelength is at 464 nm. As should be obvious, the peak of methyl orange decreases as the time increases. Thus, it is obvious that CNTs can be said as better adsorbent for methyl orange removal. Figure 7 (c) shows the MO percentage removal graph using commercial multi-walled CNTs and synthesized CNTs as an adsorbent. The MO percentage removal for both carbon nanotubes was almost similar, in which the commercial MWNTs recorded at 100 % and synthesized CNTs at 98 % after 1 hour. The synthesized CNTs high percentage removal obtained could be due to the treatment process with acids and resulting particles with high affinity for the ionic species adsorption from the aqueous solution (Li *et al*., 2013).

Defects occurred during acid treatment also could contribute to an adsorption activity enhancement. In this process, acid-oxidants attack not only the existing defect sites but also perfect sites in CNTs sidewalls and damage them to induce additional defect sites (Chiang *et al*., 2011). After treatment process, both CNTs ends were opened and only a small metal catalyst amount will remain in CNTs. This may be attributed to the electrostatic interaction between anionic dyes and partially negatives charged CNTs surface due to the oxygen-containing functional group's presence.

Another study reported that CNTs is strongly adsorbed organic pollutants due to hydrophobic interaction, hydrogen bonding, π-π interactions, covalent bonding and electrostatic interactions (Yang & Xing, 2010). For hydrophobic interaction, the CNTs sidewall has highly hydrophobic properties because of the high π electron density of sp2 carbons. So dyes may interact with CNTs sidewall through hydrophobic interactions (Yan *et al*., 2005). For hydrogen bonding, it occurred when the CNTs surface has –COOH and –OH functional groups, thus could form hydrogen bonds with the graphitic CNTs which donates electrons and would be beneficial to improve the CNTs adsorption affinity for the removal of dyes. (Yang *et al*., 2008). While π-π bonding takes place between CNTs bulk π system and dye molecules with C=C or benzene rings and electrostatic interactions greatly control the the adsorption of the ionic compound because of the charged CNT surface (Liu *et al*., 2012).

Conclusion

The synthesized CNTs grown on the Ni-MCM41 catalyst were successfully developed. The XRD, Raman, and FTIR results confirmed the synthesized CNTs obtained are multi-walled carbon nanotubes (MWNTs). Whilst, SEM images show the synthesized MWNTs appear as the hairlike structure with the diameter range between 2-5 nm and hundred nanometers in length. The synthesized MWNTs exhibit an excellent methyl orange percentage removal of 98 % after 1 hour and comparable to commercial MWNTs at 100 %.

Acknowledgements

Special thanks to the Ministry of Higher Education Malaysia for MyPhD scholarship and Fundamental Research Grant Scheme (FRGS), vot no. 55924 and 59358, School of Fundamental Science, Central Laboratory, Universiti Malaysia Terengganu and Institute of Science, Universiti Teknologi Mara for research and supports facilities.

References

Belay, K., & Hayelom, A. (2014). Removal of methyl orange from aqueous solutions using thermally treated egg shell (locally available and low cost biosorbent). *International Journal of Innovation and Scientific Research*, 8(1): 43-49.

Che, G., Lakshmi, B., Martin, C., Fisher, E., & Ruoff, R. S. (1998). Chemical vapor deposition based synthesis of carbon nanotubes and nanofibers using a template method. *Chemistry of Materials*, 10(1): 260-267.

Chiang, Y.-C., Lin, W.-H., & Chang, Y. C. (2011). The influence of treatment duration on multi-walled carbon nanotubes functionalized by h2so4/hno3 oxidation. *Applied Surface Science*, 257(6): 2401-2410.

Demirbas, A. (2008). Heavy metal adsorption onto agro-based waste materials: a review. *Journal of Hazardous Materials*, 157(2): 220-229.

Duxiao, J., Nongyue, H., Yuanying, Z., Chunxiang, X., Chunwei, Y., & Zuhong, L. (2001). Catalytic growth of carbon nanotubes from the internal surface of Fe-loading mesoporous molecular sieves materials. *Materials Chemistry and Physics*, 69(1): 246-251.

Gong, J.-L., Wang, B., Zeng, G. -M., Yang, C.-P., Niu, C.-G., Niu, Q.-Y., & Liang, Y. (2009). Removal of cationic dyes from aqueous solution using magnetic multi-wall carbon nanotube nanocomposite as adsorbent. *Journal of Hazardous Materials,* 164(2–3): 1517-1522.

Gupta, V. K., Kumar, R., Nayak, A., Saleh, T. A., & Barakat, M. (2013). Adsorptive removal of dyes from aqueous solution onto carbon nanotubes: a review. *Advances in Colloid and Interface Science*, 193: 24-34.

Herrera, J. E., Balzano, L., Borgna, A., Alvarez, W. E., & Resasco, D. E. (2001). Relationship between the structure/composition of Co–Mo catalysts and their ability to produce single-walled carbon nanotubes by CO disproportionation. *Journal of Catalysis*, 204(1): 129-145.

Ji, L., Chen, W., Duan, L., & Zhu, D. (2009). Mechanisms for strong adsorption of tetracycline to carbon nanotubes: a comparative study using activated carbon and graphite as adsorbents. *Environmental Science & Technology*, 43(7): 2322-2327.

Kobya, M., Demirbas, E., Senturk, E., & Ince, M. (2005). Adsorption of heavy metal ions from aqueous solutions by activated carbon prepared from apricot stone. *Bioresource Technology*, 96(13): 1518-1521.

Krishnamurthy, G., & Namitha, R. (2013). A novel method of synthesis of carbon nanotube by hydrothermal process. *International Journal of Science Research*, 1(4): 358-362.

Li, Y., Du, Q., Liu, T., Peng, X., Wang, J., Sun, J., & Xia, Y. (2013). Comparative study of methylene blue dye adsorption onto activated carbon, graphene oxide, and carbon nanotubes. *Chemical Engineering Research and Design*, 91(2): 361-368.

Liu, F., Chung, S., Oh, G., & Seo, T. S. (2012). Three-dimensional graphene oxide nanostructure for fast and efficient water-soluble dye removal. *ACS Applied Materials & Interfaces*, 4(2): 922-927.

Masoumi, M., Mehrnia, M. R., Montazer-Rahmati, M., & Rashidi, A. M. (2010). Templated growth of carbon nanotubes on nickel loaded mesoporous MCM-41 and MCM-48 molecular sieves. *International Journal of Nanoscience and Nanotechnology*, 6(2): 88-96.

Minamisawa, M., Minamisawa, H., Yoshida, S., & Takai, N. (2004). Adsorption behavior of heavy metals on biomaterials. *Journal of Agricultural and Food Chemistry*, 52(18): 5606-5611.

Mishra, A. K., Arockiadoss, T., & Ramaprabhu, S. (2010). Study of removal

of azo dye by functionalized multi walled carbon nanotubes. *Chemical Engineering Journal*, 162(3): 1026-1034.

Murphy, H., Papakonstantinou, P., & Okpalugo, T. T. (2006). Raman study of multiwalled carbon nanotubes functionalized with oxygen groups. *Journal of Vacuum Science & Technology B*, 24(2): 715-720.

Occelli, M., Biz, S., & Auroux, A. (1999). Effects of isomorphous substitution of Si with Ti and Zr in mesoporous silicates with the MCM-41 structure. *Applied Catalysis A: General*, 183(2): 231-239.

Pal, J., Deb, M. K., Deshmukh, D. K., & Verma, D. (2013). Removal of methyl orange by activated carbon modified by silver nanoparticles. *Applied Water Science*, 3(2): 367-374.

Potgieter, J., Potgieter-Vermaak, S., & Kalibantonga, P. (2006). Heavy metals removal from solution by palygorskite clay. *Minerals engineering*, 19(5): 463-470.

Scheibe, B., Borowiak-Palen, E., & Kalenczuk, R. (2009). Effect of the silanization processes on the properties of oxidized multiwalled carbon nanotubes. *Acta Physica Polonica A*, 116: S150-S155.

Sheikh, F. A., Macossay, J., Cantu, T., Zhang, X., Hassan, M. S., Salinas, M. E., Bowlin, G. L. (2015). Imaging, spectroscopy, mechanical, alignment and biocompatibility studies of electrospun medical grade polyurethane (Carbothane™ 3575A) nanofibers and composite nanofibers containing multiwalled carbon nanotubes. *Journal of the Mechanical Behavior of Biomedical Materials*, 41: 189-198.

Somanathan, T., Pandurangan, A., Subashini, D., & Sathiyamoorthy, D. (2006). Growth of single walled carbon nanotubes over Co-MCM-41 mesoporous molecular sieves. *Indian Journal of Pure and Applied Physics*, 44(2): 173.

Taib, N. I., Endud, S., & Katun, M. N. (2011). Functionalization of mesoporous Si-MCM-41 by grafting with trimethylchlorosilane. *International Journal of Chemistry*, 3(3): 2-10.

Tangestaninejad, S., Moghadam, M., Mirkhani, V., Mohammadpoor-Baltork, I., & Ghani, K. (2009). Alkene epoxidation catalyzed by molybdenum supported on functionalized MCM-41 containing N–S chelating Schiff base ligand. *Catalysis Communications*, 10(6): 853-858.

Wildgoose, G. G., Banks, C. E., Leventis, H. C., & Compton, R. G. (2006). Chemically modified carbon nanotubes for use in electroanalysis. *Microchimica Acta*, 152(3-4): 187-214.

Yan, Y., Zhang, M., Gong, K., Su, L., Guo, Z., & Mao, L. (2005). Adsorption of methylene blue dye onto carbon nanotubes: a route to an electrochemically functional nanostructure and its layer-by-layer assembled nanocomposite. *Chemistry of Materials*, 17(13): 3457-3463.

Yang, K., Wu, W., Jing, Q., & Zhu, L. (2008). Aqueous adsorption of aniline, phenol, and their substitutes by multi-walled carbon nanotubes. *Environmental Science & Technology*, 42(21): 7931-7936.

Yang, K., & Xing, B. (2010). Adsorption of organic compounds by carbon nanomaterials in aqueous phase: Polanyi theory and its application. *Chemical Reviews*, 110(10): 5989-6008.